Analysis and Simulation of Contact Stress Model for Elastic Wheels on Road Surface

Bo Li, Shao-yi Bei, Ting Zhou, Zhang Ni, Jing-bo Zhao, Lan-chun Zhang

School of Automobile and Traffic Engineering，Jiangsu University of Technology，Changzhou,213001，China

***Abstract* — The interaction between pneumatic wheel and ground has important influence on the performance of vehicle's operation, but for the non-pneumatic wheel, research on this aspect is less. In this paper, a contact stress model for new elastic wheel on ground is proposed. Two elastomers, ground and non-pneumatic wheel, are included in the contact model, and the vertical load is applied on the interior rigid hub of non-pneumatic wheel. The stress distribution of contact areas is emphasized on the three dimensional analysis of quasi static, and the effect of materials properties, and curvature of elastomers on maximum stress are also considered. From the analysis point of view, the maximum stress is located in the contact center, and the farther the distance from the center, the smaller the contact stress is. A complete parameters analysis of non-pneumatic wheel and ground is put forward, which can be used to support the optimization design of non-pneumatic wheel. The model was verified by the finite element software ABAQUS.**

Key words* — *Wheel; Contact stress model; Stress distribution; Parameters analysis

I. INTRODUCTION

Tyres are a key part of automobile, and the only medium in the contact with ground, which is used to support loads, transfer braking force, drive and steer, and reduce vibration. Therefore, tire has some requirements such as safety, durability, and security is particularly important [1]. Tire needs to sustain collision from the uneven roads, perforation, and other conditions, which may threaten to passengers' safety, so the non-pneumatic tire arises at the historic moment in order to meet the needs of the development of modern automobile industry. Today, the common technologies of security wheel are the following three types: Run-flat Tire [2-3], Leak-proof Tire (TUFFUP TIRE) [4]and Non-pneumatic Tire [5-8].

Numerous theoretical and computational models about soil-tire contact analysis [9-14] and dynamic analysis of pneumatic tires have been proposed[15-18]. These models are based on the theory of elastic ring, and prove effective for estimating the inherent frequency and models' deformation. But very few analysis methods for contact problems of non-pneumatic wheel have been given. Usually, numerical simulation is used to explain the problem of road contact of non-pneumatic wheel . In the case of a pure bending beam, little detailed research on tires' contact has been done from the angle of analysis. Rhyne and Cron[19] gave a simple contact model which contained a flexible ring of Michelin non-pneumatic wheel with bending and shear deformation. Recently, Gasmi et al [20] took contact model as the flexible ring on two rigid surfaces with beam model and elastic plastic theory, and focused on bearing and deforming of elastic beam, considering a little about contact problem. Genta[21] presented a kind of elastic wheel which can adapt the low gravity environment, so as to adapt the environment of strong radiation, vacuum, fragment under alien detection and other extreme situations. Rhyne and Cron[19] proved that Michelin non-pneumatic wheel was easy to copy most characteristics of pneumatic tire and exceed some. So, this kind of non-pneumatic tire can break the limitation of traditional pneumatic tire and expand the design space potentially.

Based on the above references, researchers usually focused on bearing and deforming of elastic wheel, considering a little about contact problem, and establishment of detailed contact model of tire-road is very necessary. In this paper, a new non-pneumatic wheel is different from Michelin non-pneumatic wheel, which contact stress distribution model between wheel and road based on the theory of elasticity is put forward. In Rhyne and Cron's research, a simplified calculation method of the average value of ground contact stress was put forward. The deeper contact problem is solved further in this research, such as quantitative research on relations between contact stress extreme value, curvature of ground, road surface, the influence of wheel and properties of ground's material on the contact stress. The model can be applied in lots of fields, such as cropper, bulldozer, wheelchair, automobile, military wheels, etc. The model's validation is done in finite element software ABAQUS, and some key features' parametric analysis of non-pneumatic wheel is presented, thus design space is broaden and the ability of the model is displayed.

II. SIMPLIFIED MODEL OF NEW ELASTIC NON-PNEUMATIC WHEEL

From Figure 1, the structure of new elastic non-pneumatic wheel is very different from that of traditional tires，which includes rubber ring, elastic closed belts, metal ring and rigid hub, and the elastic closed belt consists of metal fixed rings and elastic polyurethane belt. Elastic polyurethane belt is non-pneumatic elastic structure, and fixed by the metal fixed ring to the metal hub and metal ring. Elastic closed belt can be compressed by the load from

metal hub, and also have a certain lateral displacement DOF, in order to abtain excellent lateral stability.

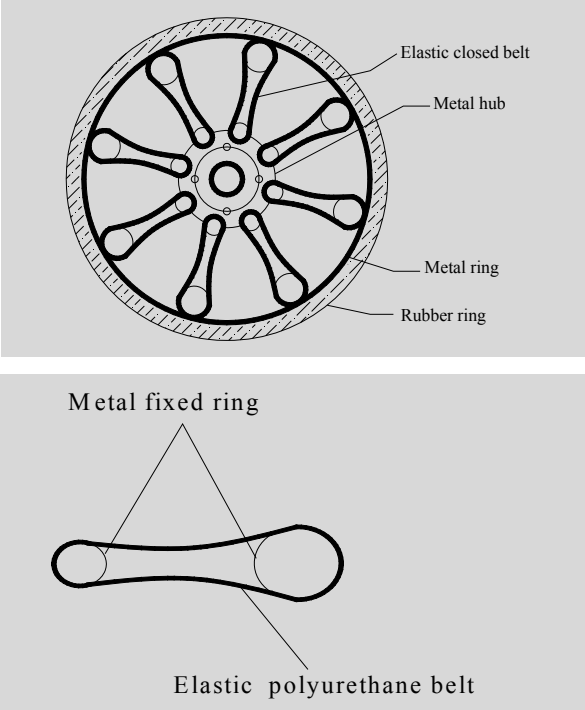

Figure 1. Structure of Elastic Non-pneumatic Wheel.

III. AVERAGE (SIMPLIFIED) CONTACT STRESS OF THE SIMPLIFIED MODEL

The structure and load characters of Michelin non-pneumatic wheel are as Figure 2,

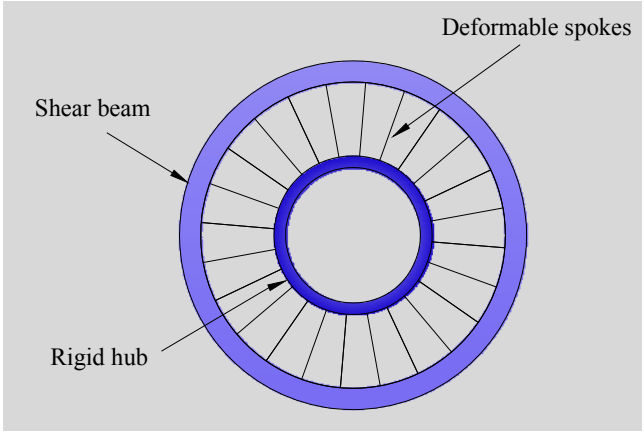

Figure 2. Structure and Load Character of Michelin Non-pneumatic Wheel.

According to the theory of elasticity(Figure 3) that the shear deformation occurs when Michelin non-pneumatic wheel is under static load. The shear strain λ_{xz} can be written as[19],

$$\lambda_{xz}=\tan^{-1}(\frac{(r+h)\theta-r\theta}{h})=\tan^{-1}(\frac{h\theta}{h})=\tan^{-1}(\theta) \quad (1)$$

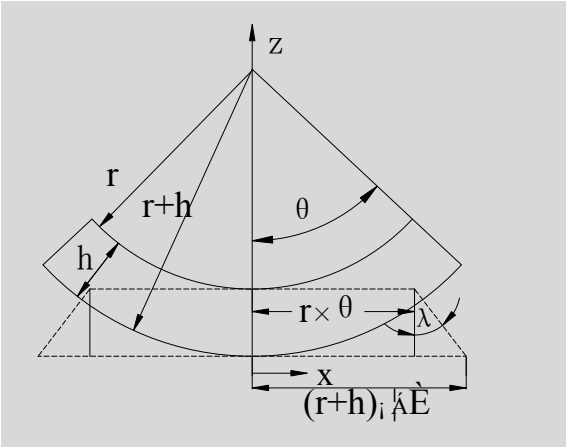

Figure 3. Length of a Shear Beam Deformed to a Flat Surface

Using that $x=R\theta$, the shear strain from Eqs. (1) becomes,

$$\lambda_{xz}=\tan^{-1}(\frac{x}{R}) \quad (2)$$

Assuming the composite shear modulus is *G*, the shear stress can be obtained by Eqs.(3),

$$\sigma_{xz} = G\lambda_{xz} = G\tan^{-1}(\frac{x}{R}) \tag{3}$$

Consider the vertical stress distribution of an infinitesimal length of the wheel outer ring and assuming that the contact stress is *p* and the stress distribution coordinate system is the same as in Fig.2, summing the forces in the z direction yields,

$$(\sigma_{xz} + \frac{\partial \sigma_{xz}}{\partial x}dx)h - \sigma_{xz}h - pdx = 0 \tag{4}$$

Solving Eqs. (4) for the contact stress gives,

$$p = \frac{\partial \sigma_{xz}}{\partial x}h \tag{5}$$

We know the shear stress from Eqs.(3) and can differentiate the contact stress with respect to *x*, then Eqs.(5) becomes,

$$p = G\frac{1}{R(1+\frac{x^2}{R^2})}h = \frac{Gh}{R+\frac{x^2}{R}} \tag{6}$$

Then the contact stress of different contact area can be obtained from Eqs.(6). If the half contact length *x* is small relative to the radius *R*, $\frac{x^2}{R} \approx 0$, Eqs.(6) can be approximately simplified as,

$$p \approx \frac{Gh}{R} \tag{7}$$

Thus, we can approximately estimate the contact stress between the wheel and road surface.

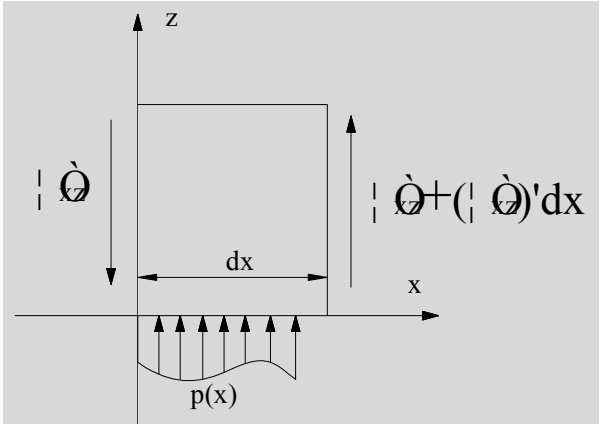

Figure 4. The Vertical Stress Distribution of an Infinitesimal Length of the Wheel Outer Ring

The model is too simplified, for example, some forces and couples of cross section are removed, and which can be solved is the average contact stress between wheel and ground. The actual contact stress distribution and maximum stress cannot be obtained, so a more detailed and accurate model for analysis needs to be built.

IV. CONTACT STRESS OF THE ACCURATE MODEL

Assume the contact between ground and wheel as the contact between elastomers[22]. Take the contact point *O* before transformation as the original point of coordinates, and public tangent plane as *Oxy* plane, as shown in Figure 5. Elastomer's curved surface near the contact point can be expressed by the following general form:

$$\begin{aligned} Q_1 &= E_1(x, y) \\ Q_2 &= E_2(x, y) \end{aligned} \tag{8}$$

Expand $E_1(x, y)$ and $E_2(x, y)$ to Taylor series at contact point's neighborhood. The original point of coordinates is at contact point, and *Oxy* plane is public tangent plane at the contact point of two bodies, so constant term and the first power term are not included in the series, and the first item of series is quadratic term. The stress and deformation of the contact area and its nearby are mainly studied in the paper, so the third power and over are removed. Hence, two curved surfaces around the contact point can be approximately expressed as follows.

$$\begin{aligned} Q_1 &= (A_1x + A_2y)x + A_3y^2 \\ Q_2 &= (B_1x + B_2y)x + B_3y^2 \end{aligned} \tag{9}$$

The distance between P_1 and P_2 is

$$Q_1 + Q_2 = [(A_1 + B_1)x + A_2y]x + [B_2x + (A_3 + B_3)y]y \tag{10}$$

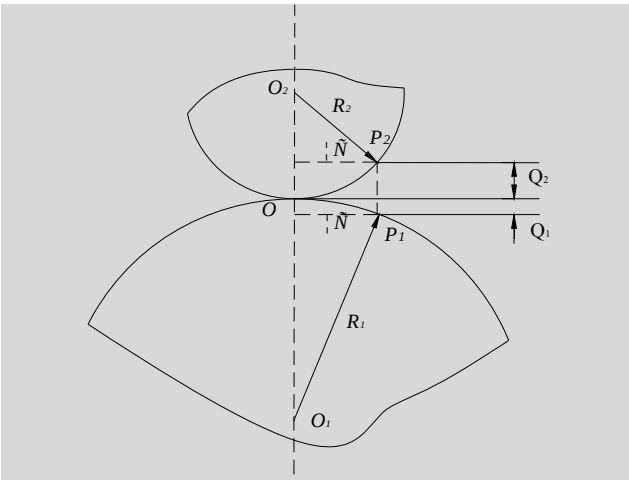

Figure 5. Contact of Two Two-dimensional Circles

Then, it is necessary to prove that when the axle Oz does not change, the item *xy* in Eqs.(10) can zeroing by twirling axles. Therefore, use $\frac{1}{R_1}$ and $\frac{1}{R_{11}}$ to express the main curvatures at the contact point O of elastomers surface(suppose $R_1 < R_{11}$), and take the corresponding direction of two main curvatures as the direction of axles *Ox*1 and *Ox*2. Then, the curved surface in the small field around the contact point can be expressed as: $Q_1 = \frac{x_1^2}{2R_1} + \frac{y_1^2}{2R_{11}}$ Similarly, to the above elastomers, if using $\frac{1}{R_2}$ and $\frac{1}{R_{21}}$ to express the main curvatures at the contact point(suppose $R_2 < R_{21}$), and taking the corresponding direction of two main curvatures as the direction of axles Ox2 and Oy2, the curved surface in the small field around the contact point can be expressed as:

the distance between P_1 and P_2 is

$$Q_1 + Q_2 = \frac{x_1^2}{2R_1} + \frac{x_2^2}{2R_2} + \frac{y_1^2}{2R_{11}} + \frac{y_2^2}{2R_{21}} \tag{11}$$

With the introduction of the new coordinate system $Ox_{11}y_{11}$, the transformation relationship is existed as follows:

$$\begin{cases} x_1 = x_{11}\cos\phi_1 - y_{11}\sin\phi_1 \\ x_2 = x_{11}\cos\phi_2 - y_{11}\sin\phi_2 \\ y_1 = x_{11}\sin\phi_1 + y_{11}\cos\phi_1 \\ y_2 = x_{11}\sin\phi_2 + y_{11}\cos\phi_2 \end{cases} \tag{12}$$

Substitute Eqs.(5) into Eqs.(4),

$$\begin{aligned} Q_1+Q_2 &= y_{11}^2[\frac{1}{2R_1}\sin^2\phi_1+\frac{1}{2R_2}\sin^2\phi_2+\frac{1}{2R_{11}}\cos^2\phi_1+\frac{1}{2R_{21}}\cos^2\phi_2] \\ &+x_{11}^2[\frac{1}{2R_1}\cos^2\phi_1+\frac{1}{2R_2}\cos^2\phi_2+\frac{1}{2R_{11}}\sin^2\phi_1+\frac{1}{2R_{21}}\sin^2\phi_2]+ \\ &-x_1y_1[(\frac{R_{11}-R_1}{2R_1R_{11}})\sin2\phi_1+(\frac{R_{21}-R_2}{2R_2R_{21}})\sin2\phi_2] \end{aligned} \tag{13}$$

In order to cancel the item x_1y_1 , the only way is zero its coefficient, that is Substitute Eqs.(4) into the above equation and calculate,

$$\tan2\phi_1 = \sin2\phi(\frac{R_{21}-R_2}{R_2R_{21}}) \Big/ (\frac{R_{21}-R_2}{R_2R_{21}})\cos2\phi+(\frac{R_{11}-R_1}{R_1R_{11}}) \tag{14}$$

Supposing that the condition meet and replace x_1 and y_1 in Eqs.(6) with x and y , that is to choose the coordinate system for the requirement that the item *x y* does not appear at the beginning. In addition,

$$\begin{aligned} 2A &= \frac{(R_{11}R_2R_{21}\cos^2\phi_1+R_1R_2R_{21}\sin^2\phi_1+R_1R_{11}R_{21}\cos^2\phi_2+R_1R_{11}R_2\sin^2\phi_2)}{R_1R_{11}R_2R_{21}} \\ 2B &= \frac{(R_{11}R_2R_{21}\sin^2\phi_1+R_1R_2R_{21}\cos^2\phi_1+R_1R_{11}R_{21}\sin^2\phi_2+R_1R_{11}R_2\cos^2\phi_2)}{R_1R_{11}R_2R_{21}} \end{aligned} \tag{15}$$

Then the equation is simplified to $Q_1 + Q_2 = Ax^2 + By^2$. Add and subtract two equations in Eqs.(15),

$$2A+2B=\frac{R_{11}R_2R_{21}+R_1R_2R_{21}+R_1R_{11}R_{21}+R_1R_{11}R_2}{R_1R_{11}R_2R_{21}}$$

$$2A-2B=\frac{R_{11}-R_1}{R_1}\cos 2\phi_1+\frac{R_{21}-R_2}{R_2R_{21}}\cos 2\phi_2 \tag{16}$$

For a given problem, R_1, R_{11}, R_2, R_{21} and ϕ are known, so A and B can be obtained from Eqs.(16). Q_1+Q_2 is always positive, so A and B are always positive too. It can be seen that the boundary of the contact surface is ellipse obviously, which is the superposition of points with equivalence Q_1+Q_2 in two elastic bodies after partial transformation. Supposing that α, λ_1 and λ_2 have the same meaning with the time when two spheres contact each other, so from geometrical relationship,

$$\lambda_1+\lambda_2=\alpha-(Q_1+Q_2)=\alpha-Ax^2-By^2 \tag{17}$$

So

$$\lambda_1+\lambda_2=\iint\frac{q(u,v)}{\rho}dudv\frac{(1-v_1^2)e_2+(1-v_2^2)e_1}{\pi e_1e_2} \tag{18}$$

where, $\rho=\sqrt{(x-u)^2+(y-v)^2}$ is the distance between any point（u,v）in the contact surface and the specified point （x,y）in the contact surface, substitute Eqs.(18) into Eqs.(17),

$$(c_1+c_2)\iint\frac{q}{\rho}dudv=\alpha-Ax^2-By^2 \tag{19}$$

Where, $c_1=\frac{1}{e_1\pi}-\frac{v_1^2}{e_1\pi}$, $c_2=\frac{1}{e_2\pi}-\frac{v_2^2}{e_2\pi}$, the problem of solving the stress on two contact surfaces is boiled down to solve the integral equation (19). A half ellipsoid is made based on the contact surface (the perimeter is ellipse and two semiaxises are respectively a and b). Then, it is verified that the stress on the contact surface is proportional to the vertical coordinate of the ellipsoid, namely,

$q(u,v)=\frac{q_0}{ab}\sqrt{a^2b^2-u^2b^2-a^2v^2}$. where, q_0 is the stress of central point O. From equilibrium conditions, the volume of a half ellipsoid is equivalent to total stress F, namely, $F=\iint qdudv=\frac{2}{3}\pi abq_0$. Thus, $q_0=\frac{3F}{2\pi ab}$. The distribution of contact stress on the contact surface is $q(u,v)=\frac{3F}{2\pi a^2b^2}\sqrt{a^2b^2-b^2u^2-a^2v^2}$. The results a and b are as follows:

$$\begin{cases}a=\sqrt[3]{\frac{3\pi p_1^3}{4}[\frac{F(c_1+c_2)}{(A+B)}]}\\ b=\sqrt[3]{\frac{3\pi p_2^3}{4}[\frac{F(c_1+c_2)}{(A+B)}]}\end{cases} \tag{20}$$

If two elastomers are spheres, $R_1=R_{11}$, $R_2=R_{21}$, $A=B$, where $p_1=p_2=1$. Then Eqs.(13) turns into $a=b=\sqrt[3]{\frac{3\pi F(c_1+c_2)R_1R_2}{4(R_1+R_2)}}$. Maximum stress is $q_0=\frac{3F}{2\pi a^2}$, namely,

$$q_0=\frac{3F}{2\pi}[\frac{4(R_1+R_2)}{3\pi F(k_1+k_2)R_1R_2}]^{\frac{2}{3}} \tag{21}$$

Assuming that the contact between wheel and ground is the contact between sphere and plane (Figure.6a), that is $R_1\to\infty$, and then the required results can be obtained. To assume that the contact between wheel and concave-convex ground is the contact between sphere and foundation of

sphere (Figure.6b), Making R_1 negative is the only thing we need to do.

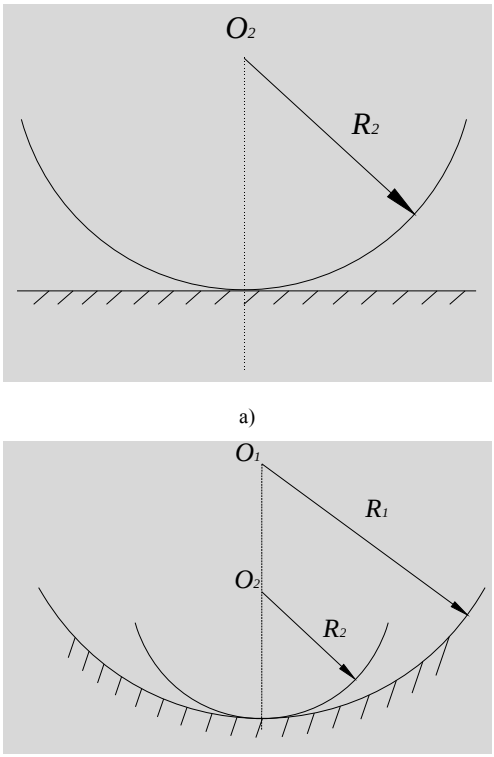

Figure 6. Simplified Contact Model between Wheel and Ground.

V. VALIDATION

A. Numerical Validation

The original constraint of elastic wheel model is relatively complex, and there exists many structural lines, variable curvature surfaces, rounding, small embossments and depressions, which have great influence on the meshing quality of the model, and even on the correctness of the analysis results. For mesh generation, the model needs to be simplified, and structural constitution which does not affect simulation analysis are removed or modified. Wheel hub are regarded as rigid bodies approximately, regardless of its deformation, which have played a role in the force transmission only, so which can be removed, and constraints and static load forces are directly added to the elastic outer ring of the wheel. Meanwhile, there are curtain with beam layer and other structures in the wheels' outer ring, whose material is complex. Thus, the wheels' outer ring can be simplified into two layers of binding contact with each other, ignoring connection structure of the elastic ring and the elastic combination card and the effect of reset springs. Then the wheels' outer ring is simplified into the stackable structural style between frame layer and elastic layer.

The simplified model of elastic wheel is built in the analytics software ABAQUS, the material properties of every part are set in Table 1, hexahedral element model is get by using sweeping meshing, and grid's quality control is done. Then, the finite element model of elastic wheel is obtained.

TABLE □. WHEEL PROPERTY USED FOR THE PURPOSE OF VALIDATION

Material Parameters		**Geometrical Parameters**			
e_2(MPa)	**v_2**	**R_2(m)**		h(m)	F(N)
1.5	0.49	0.48		0.08	4800

From Figure 7 and 8, the contact stress's distribution given by the finite element software ABAQUS is consistent with numerical analysis result，and maximum stress from two methods is very close to each other，so this analysis model has very good adaptability.

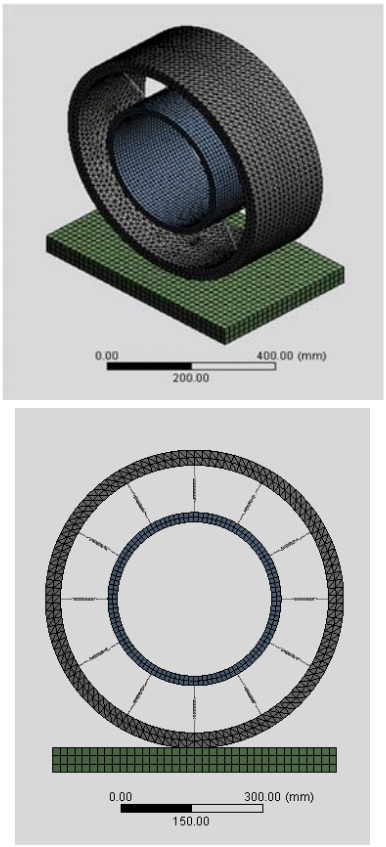

Figure 7. Finite Element Model

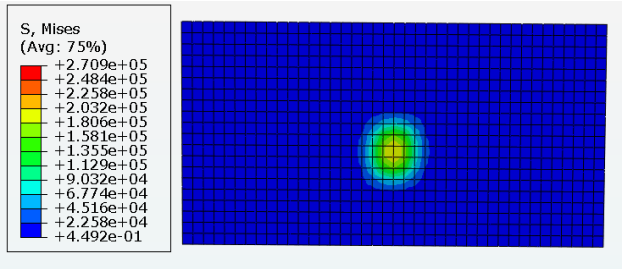

a) Simulation results

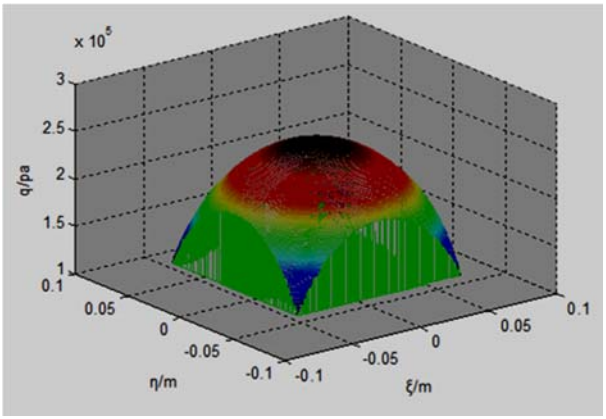

(b)theoretical caculation

Figure 8. Comparison between Simulation and Theoretical Calculation of Ground Contact Stress.

Under normal conditions, the radius of ground surface $R_1 \to \infty$, but in the case of a spurious ground surface, R_1 changes very little. Changes of maximum stress of contact surface q_0 are discussed (Figure 9),

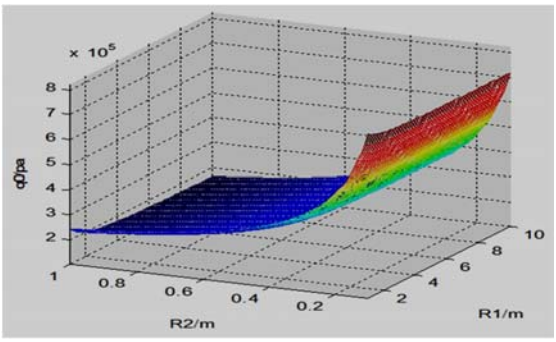

Figure 9. Relationship between Maximum Stress of Ground Surface and R_1,R_2

where R_1 ranges from 1m to 10m, and R_2 ranges from 0.1m to 1m.

In different grounds, $c_1 = \dfrac{1-v_1^2}{\pi e_1}$ changes very much. Similarly, for elastic wheels, $c_2 = \dfrac{1-v_2^2}{\pi e_2}$ also changes along with roads' conditions. So the changes' relationship between c_1, c_2 and q_0 is shown in Figure 10. Relationships between c_1, v_1 and e_1, c_2, v_2 and c_2 are shown in Figure 11.

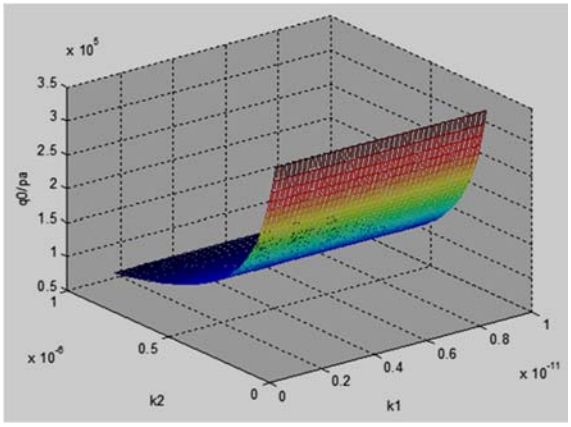

Figure 10. Relationship between Maximum Stress of Contact Surface and C_1,C_2

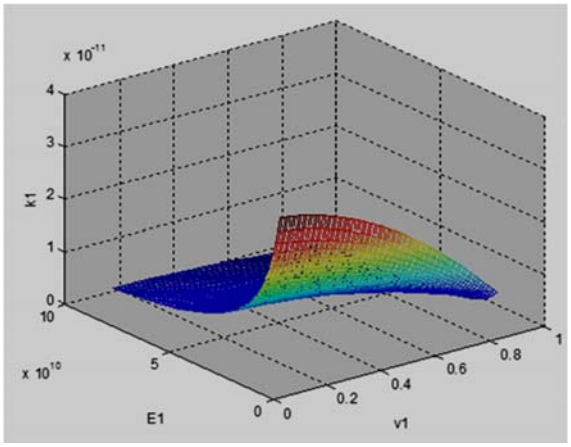

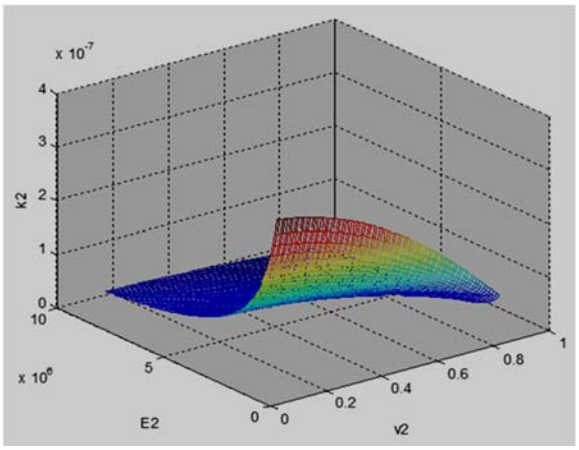

Figure 11. Relationship between c, v and e

VI. CONCLUSIONS

Based on a large number of literature on tire contact model，the exact contact model between a new non-pneumatic wheel and ground has been considered, where contact surface is frictionless and static load is applied on the rigid hub of wheel. The model takes into account the stress distribution of contact area, and some key model parameters. In addition, their relationship is shown clearly in three-dimensional graphs. The solution shows the maximum stress is located in the contact center, and the farther the distance from the center is, the smaller the contact stress is. Three-dimensional numerical simulation results are acquired by finite element software ABAQUS. These two types of results are consistent with theoretical analysis from the graph of pressure distribution, which shows how the model is effective under static condition. The detailed contact model between wheel and road can be an approach for the study and design of non-pneumatic wheel.

ACKNOWLEDGMENTS

The research described in this paper was financially supported by National Natural Science Foundation of Youth Fund Project(51305175, 61503163) and Jiangsu Province"333 project" training funded project (BRA2015365).

REFERENES

[1] JD Zhuang. Advanced technology of tire. Beijing: Beijing Institute of Technology Press, 2001, pp. 1-2.
[2] Laske R F, Losey R A, Gobinath T, et al. Self-Supporting Pneumatic Tire: U.S. Patent Application 12/955,097 [P]. 2010-11-29.
[3] Seradarian P, Pelletier B. Elastomeric Insert for Supporting a Tire and Mounted Assembly Incorporating It: U.S. Patent Application 13/252,635 [P]. 2011-10-4.
[4] Asanuma N, Kawai M, Takahashi A, et al. Intelligent Technologies of ASV (The Research and Development of ASV-2 in HONDA) [C]. Proceedings of the 7TH World Congress on Intelligent Systems. 2000:1-12.
[5] Narasimhan A, Ziegert J, Thompson L. Effects of Material Properties on Static Load-deflection and Vibration of a Non-pneumatic Tire During High-speed Rolling [J]. SAE International Journal of Passenger Cars-Mechanical Systems 2011, 4(1): 59-72.
[6] Jang I G, Sung Y H, Yoo E J, et al. Pattern Design of a Non-pneumatic Tyre for Stiffness Using Topology Optimization[J]. Engineering Optimization 2012, 44(2): 119-131.
[7] Bras B, Cobert A. Life-Cycle Environmental Impact of Michelin Tweel® Tire for Passenger Vehicles[J]. SAE International Journal of Passenger Cars-Mechanical Systems 2011, 4(1): 32-43.
[8] Cardile D, Viola N, Chiesa S, et al. Applied Design Methodology for Lunar Rover Elastic Wheel[J]. Acta Astronautica 2012, 81(1): 1-11.
[9] Nguyen VN, Matsuo T, Inaba S, Koumoto T. Experimental analysis of vertical soil reaction and soil stress distribution under off-road tires. J Terramech 2008;45:25-44.
[10] Fervers CW. Improved FEM simulation model for tire-soil interaction. J Terramech 2004;41:87-100.
[11] Carman K. Prediction of soil compaction under pneumatic tires using fuzzy logic approach. J Terramech 2008;45:103-8.
[12] Nakashima H, Oida A. Algorithm and implementation of soil-tire contact analysis code based on dynamic FE-DE method. J Terramech 2004;41:127-37.
[13] Pacejka HB, Sharp RS. Shear force development by pneumatic tyres in steady state conditions:a review of modeling aspects. Vehicle Syst Dyn 1991;20:121-76.
[14] Sjahdanulirwan M. Yang Q. Prediction of tyre-road friction with an inverted-boat shaped stress distribution. Vehicle Syst Dyn 1995;24:145-61.
[15] Guo K, Lu D. UniTire: unified tire model for vehicle dynamic simulation[J]. Vehicle System Dynamics, 2007, 45(S1): 79-99.
[16] Xu N, Guo K, Zhang X. UniTire Model for Tire Forces and Moments under Combined Slip Conditions with Anisotropic Tire Slip Stiffness[J]. SAE International Journal of Commercial Vehicles, 2013, 6(2): 315-324.
[17] Guo K, Lu D, Chen S, et al. The UniTire model: a nonlinear and non-steady-state tyre model for vehicle dynamics simulation[J]. Vehicle system dynamics, 2005, 43(sup1): 341-358.
[18] Gim G. An analytical model of pneumatic tires for vehicle dynamic simulations. Part 1[J]. Int. J. Vehicle Des., 1990, 11: 589-618.
[19] Rhyne, T.B., Cron, S.M. Development of a non-pneumatic wheel. Tire Sci.Technol 2006. 34, 150-169.
[20] Gasmi, A.,Joseph, P.F.,Rhyne, T.B.,Cron, S,M. Closed-form solution of a shear deformable, extensional ring in contact between two rigid surfaces. Int. J. Solids Struct 2011.48,843-853.
[21] Genta, G.,Genta, A. Modeling and Nonlinear Analysis of an Elastic Wheel for Low-Gravity Application. XXXVIII Conv. Naz. AIAS, Torino. Available from: <http://www.giancarlogenta.it/Pubblicazioni.htm>.
[22] JL Wu. Elasticity . Beijing: Higher Education Press, 2011, pp. 244-251.d3

APPENDIX

θ/(°)	p_1	p_2
18	4.156	0.394
20	3.850	0.410
25	3.152	0.456
30	2.731	0.493
35	2.937	0.530
40	2.136	0.567
45	1.926	0.604
50	1.754	0.641
55	1.611	0.678
60	1.486	0.717
65	1.378	0.759
70	1.284	0.802
75	1.202	0.846
80	1.128	0.893
85	1.061	0.944
90	1.000	1.000